PHYSICAL REVIEW E **78**, 010201(R) (2008)

Shear-rate-dependent structural order and viscosity of a fluid with short-range attractions

William P. Krekelberg,[1] Venkat Ganesan,[1,2] and Thomas M. Truskett[1,2,*]
[1]*Department of Chemical Engineering, University of Texas at Austin, Austin, Texas 78712, USA*
[2]*Institute for Theoretical Chemistry, University of Texas at Austin, Austin, Texas 78712, USA*
(Received 12 May 2008; published 28 July 2008)

We study a model short-range attractive fluid under shear. For this system, the strength of interparticle attractions strongly influences the equilibrium structural order. We find that shear monotonically decreases structural order regardless of the strength of the attractions. There is a strong correlation between shear-rate-dependent viscosity and a structural order metric, suggesting a structurally based constitutive equation. This correlation also holds for the Lennard-Jones fluid.

DOI: 10.1103/PhysRevE.78.010201 PACS number(s): 66.20.Cy, 61.20.Ja, 83.10.Rs

Shearing a fluid impacts both its transport coefficients and its stationary interparticle correlations. However, are shear-induced changes to dynamics and structure linked in a simple way? In the case of equilibrium fluids, the search for structure-property relations using molecular simulations and experiments has proved fruitful. For example, motivated in part by earlier studies of [1,2], researchers have found that the effects of isochoric cooling or confinement on the self-diffusion coefficient D of a number of dense model fluids can be approximately described by empirical relations of the form $\ln(DT^{-1/2}) \propto s^{\mathrm{ex}}$, where T is the temperature and s^{ex} is the molar excess entropy [1–13]. The excess entropy is a negative quantity that characterizes the number of states rendered inaccessible to an equilibrium fluid (relative to an ideal gas) due to the presence of interparticle correlations. Thus, $-s^{\mathrm{ex}}$ can be viewed as a structural order metric [14].

The link to traditional structural measures follows when s^{ex} is expressed as a sum over integral contributions from two-, three-, …, and higher-body correlation functions [15]. Several studies (see, e.g., [3,5,6,10]) have shown that the two-body contribution to the excess entropy s_2, which depends solely on the number density ρ and the pair-correlation function (PCF) $g(\mathbf{r})$, also correlates with the transport properties of dense equilibrium fluids over a range of conditions; i.e., $\ln(DT^{-1/2}) \propto s_2$ and $\ln(\eta_0 T^{-1/2}) \propto -s_2$, where η_0 is the zero-shear viscosity of the fluid. To date, however, with the exception of exact virial-like relations between shear-distorted structure and viscosity (see, e.g., [16,17]), the search for similar relationships between dynamical and structural properties of driven or out-of-equilibrium fluid systems has received comparatively little attention [18–23]. Here, we investigate via molecular dynamics simulations the relationship between shear-rate-dependent structural order, as quantified by $-s_2$, and shear viscosity.

The system we focus on is a model colloidal fluid with short-ranged attractive (SRA) interactions. In this context, "short-ranged" means a few percent of a particle diameter. SRA fluids show nontrivial structural and dynamic properties, even in the absence of shear. Whereas the mobility of a simple atomic fluid generally decreases when it is cooled, the mobility of a dense SRA fluid displays a maximum as a function of T^{-1} (or strength of the attractive interparticle interaction). Consistent with this unusual behavior, dense SRA fluids can vitrify not only upon cooling, forming an "attractive" glass or gel, but also upon heating, forming a "repulsive" or hard-sphere glass [24–30]. The precursor supercooled fluids near these two different glass transitions have different types of local structural order [10,31]. In fact, whereas $-s_2$ of a simple atomic fluid monotonically increases upon cooling, the structural order of an SRA fluid displays a minimum as a function of T^{-1} or strength of the interparticle attractions [10,31]. Qualitatively, this minimum corresponds to the intermediate states between two limits: weak interparticle attractions, where the fluid exhibits hard-sphere-like "packing order," and strong interparticle attractions, where the fluid displays gel-like "bonding order." Here, we examine how shear impacts SRA fluids with different interparticle attractions and, thus, different equilibrium structures and viscosities. In particular, we investigate whether shear-induced changes to structure for these various fluids relate in a simple way to the corresponding changes in shear viscosity.

The model SRA fluid we consider qualitatively describes a solution of colloidal particles attracted to one another by depletion interactions due to the presence of (implicit) nonadsorbing polymers. The details of the colloidal pair potential are provided in [32,33], but we discuss the main attributes below. The colloids are spherical and their effective interactions consist of three parts $U(r)=U_{\mathrm{HS}}(r)+U_{\mathrm{AO}}(r)+U_{\mathrm{R}}(r)$. (i) A strongly repulsive contribution $U_{\mathrm{HS}}(r)=k_{\mathrm{B}}T(2a_{12}/r)^{36}$, where $2a_{12}$ is the colloid diameter and k_{B} is Boltzmann's constant. (ii) An Asakura-Oosawa potential $U_{\mathrm{AO}}(r)$, which accounts for polymer-induced depletion attractions [34,35]. The strength of this attraction is approximately proportional to the volume fraction of polymers in solution ϕ_{p}, while the range is controlled by the radius of gyration of the polymers, set at $a/5$. (iii) A long-range, soft repulsion U_{R} which prevents fluid-fluid phase separation [32]. The particle radii are weakly polydisperse (drawn from a uniform distribution with mean a and half-width $a/10$) to prevent crystallization. We neglect any effects that shear might have on the effective interparticle pair potential. To simplify notation, quantities reported for this model are implicitly nondimensionalized by appropriate combinations of the characteristic length scale, the particle radius a, and the characteristic time scale $a\sqrt{m/k_{\mathrm{B}}T}$, where m is particle mass.

*Corresponding author. truskett@che.utexas.edu

We perform both equilibrium molecular dynamics (EMD) and nonequilibrium molecular dynamics (NEMD) simulations. Details of the EMD simulations are the same as those reported in [36]. Zero-shear viscosity η_0 is calculated from the EMD simulations using the Einstein form [37] of the generalized Green-Kubo relationship [38]. Several independent simulations were run at each state point to estimate the error associated with η_0.

To study this system under shear, the Newtonian equations of motion are replaced by the so-called SLLOD equations of motion [39] supplemented by Lees-Edwards boundary conditions (for details, see [40]). We employ a cubic simulation cell with $N=1000$ particles and time step $\delta t=0.001$. The applied velocity field is in the x direction, and the gradient $\dot{\gamma}$ is in the z direction ($\dot{\gamma}=dv_x/dz$). Constant T is ensured by using the isokinetic thermostat [41]. We study the shear-rate-dependent viscosity $\eta(\dot{\gamma})\equiv -P_{xz}(\dot{\gamma})/\dot{\gamma}$, where P_{xz} is the xz component of the pressure tensor. All simulations of the SRA fluid are carried out at a colloid volume fraction $\phi_c=4\pi\Sigma_i^N a_i^3/3V$ of 0.4 and polymer concentrations ϕ_p in the range 0.0–0.4. We vary shear rate $\dot{\gamma}$ between 0.001 and 0.5. All simulations were run with $k_BT=1$.

For each system, we calculate the two-body structural order parameter $-s_2$, defined as

$$-s_2 \equiv \frac{\rho}{2}\int d\mathbf{r}\{g(\mathbf{r})\ln g(\mathbf{r}) - [g(\mathbf{r})-1]\}. \tag{1}$$

For the NEMD simulations, the radial and angular dependences of the particle-averaged PCF [i.e., $g(\mathbf{r})=g(r,\theta,\phi)$] are considered. We also investigated the cumulative order integral I_{s_2} [10]:

$$I_{s_2}(r) \equiv \frac{\rho}{2}\int_0^r dr'\int_0^{2\pi} d\theta\int_0^{\pi} d\phi r'^2 \times\sin(\phi)\{g(r',\theta,\phi)\ln g(r',\theta,\phi) - [g(r',\theta,\phi)-1]\}. \tag{2}$$

As defined, $I_{s_2}(r)\to -s_2$ as $r\to\infty$. $I_{s_2}(r)$ quantifies how interparticle correlations on length scales less than r impact the structural order.

Figure 1 displays the shear-rate-dependent viscosity $\eta(\dot{\gamma})$ for fluids with different polymer concentration, ϕ_p. Consistent with earlier simulations of this system [42,43], the zero-shear viscosity η_0 has a nonmonotonic dependence on ϕ_p (see inset to Fig. 1). Interestingly, this nonmonotonic dependence occurs for all shear rates examined in this work; i.e., shear does not remove the anomalous effect that ϕ_p has on the shear viscosity. For all values of ϕ_p except the highest studied here ($\phi_p=0.4$), the fluid displays a Newtonian regime at low shear. For higher shear rates, the fluid shear thins. As might be expected, the degree of shear thinning increases with η_0. As noted elsewhere [23], this rheological behavior is largely consistent with simulations of other glass formers [44] and experimental data of SRA colloidal suspensions [45].

How does shear effect structural order? Figure 2(a) displays $-s_2$ as a function of shear rate for the values of ϕ_p studied. Similar to η, there is a clear nonmonotonic dependence of $-s_2$ on ϕ_p for all shear rates; i.e., the nontrivial effect of interparticle attractions on the structural order of the fluid is not erased by shear flow. Moreover, and also consistent with the behavior of η, the application of shear has the effect of reducing the degree of structural order in the fluid, and the amount of shear induced disordering increases with the value of $-s_2$ in the equilibrium fluid.

To explore the origins of these trends, $I_{s_2}(r)$ and, for ref-

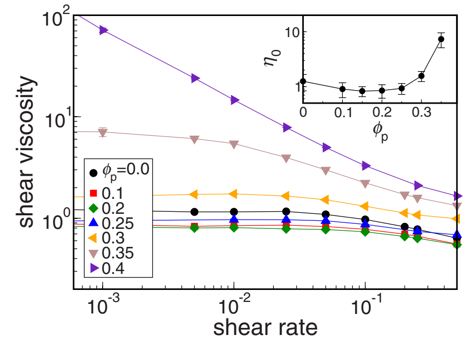

FIG. 1. (Color online) Shear viscosity versus shear rate for the model colloid-polymer system at several polymer volume fractions ϕ_p. Lines are guides to the eye. Inset shows zero-shear viscosity η_0 versus polymer concentration ϕ_p.

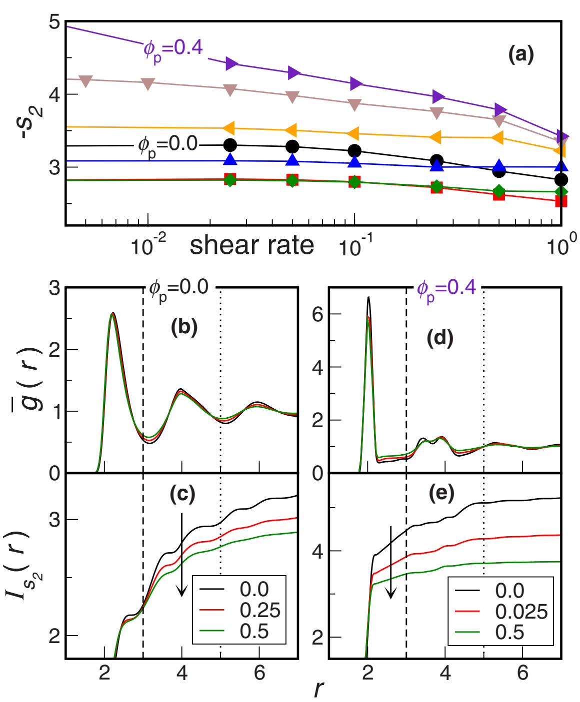

FIG. 2. (Color online) (a) Structural order metric $-s_2$ of the colloid-polymer model versus shear rate for several polymer volume fractions ϕ_p. Symbols are the same as in Fig. 1. (Lower panel) Orientationally averaged PCF $\bar{g}(r)$ and cumulative order integral $I_{s_2}(r)$ for several shear rates and two polymer concentrations: (b), (c) $\phi_p=0.0$ and (d), (e) $\phi_p=0.4$. $I_{s_2}(r)$ is calculated from the total PCF $g(\mathbf{r})$, *not* $\bar{g}(r)$. In lower panels, arrows indicate increasing shear rate; numbers in legends indicate value of shear rate; vertical dashed line is at $r=3a$ and vertical dotted line is at $r=5a$, the approximate locations of the first and second minima in $\bar{g}(r)$, respectively.

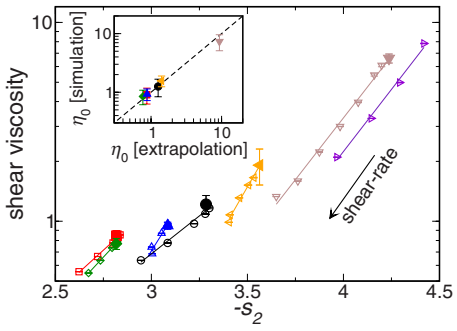

FIG. 3. (Color online) Main panel: shear viscosity versus order parameter $-s_2$ for the model colloid-polymer system. Arrow indicates increasing shear rate. Large solid symbols represent the data at zero shear. Symbols are the same as in Fig. 1. Lines are fits of the nonequilibrium data to Eq. (3). Inset: zero-shear viscosity obtained by equilibrium simulations versus that obtained from extrapolation based on $-s_2$ (see text).

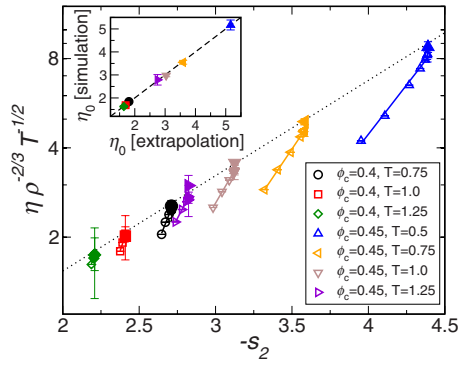

FIG. 4. (Color online) Main panel: shear viscosity versus order parameter $-s_2$ of the Lennard-Jones fluid at several values of temperature T and packing fraction ϕ_c. Large solid circles represent the data at zero shear. Solid lines are fits of the nonequilibrium data to Eq. (3). Inset: zero-shear viscosity obtained by equilibrium simulations versus those obtained from extrapolation based on $-s_2$ (see text).

erence, the orientationally averaged PCF $\bar{g}(r)$ are shown as a function of shear rate for two cases: (a) $\phi_p=0.0$ [no attractions, Figs. 2(b) and 2(c)] and (b) $\phi_p=0.4$ [strong attractions, Figs. 2(d) and 2(e)]. These plots provide insights into the specific changes in coordination shell structure that explain the shear induced disordering in these two limits.

As might be expected, in the absence of interparticle attractions ($\phi_p=0$), the model suspension has a structure similar to that of a dense, equilibrium hard-sphere fluid. In other words, first, second, and third coordination shells are well defined [see Fig. 2(b)] and make significant contributions to the overall structural order [Fig. 2(c)]. Qualitatively, the effect of shear on the PCF is to weaken those correlations (make the peaks less pronounced), although the changes to $\bar{g}(r)$ are rather minor. Nonetheless, Fig. 2(c) illustrates that even small changes have a significant impact on the integral structural order, mostly by breaking up the hard-sphere "packing order" of the second and third coordination shells.

As can be seen in Fig. 2(d), strong interparticle attractions ($\phi_p=0.4$) give rise to short-range physical bonds between the particles [10,30,31,36,46,47]. There is a pronounced first peak in the PCF and weaker second and third peaks as compared to the $\phi_p=0$ case; i.e., most of the structural order in the equilibrium fluid is due to correlations of particles with their nearest neighbors [see Fig. 2(e)]. Focusing on $\bar{g}(r)$, the effect of applying shear is to reduce the height of the first peak (i.e., breaking the physical bonds), but again the magnitude of the shear-induced changes to the PCF appears rather small. Nonetheless, the behavior of $I_{s_2}(r)$ shows that the shear-induced disordering of the first coordination shell indeed has a significant impact on the structural order of the fluid.

The data in Figs. 1 and 2(a) suggest that the effects of shear on viscosity and structural order are similar. Figure 3 displays the shear viscosity as a parametric function of $-s_2$. For a given ϕ_p and ϕ_c, the data appear to follow a relationship of the form

$$\ln[\eta(\dot{\gamma})] \propto -s_2(\dot{\gamma}). \tag{3}$$

The lines in Fig. 3 show the fits of the nonequilibrium data to Eq. (3). This relationship can be viewed as a structurally based constitutive equation. Recall that, by our choice of nondimensionalization, the viscosity is implicitly scaled by $T^{-1/2}$. Equation (3) is therefore qualitatively similar to the structure-property relation obeyed for the equilibrium fluid.

There are two simple potential uses for for such a relationship. Like other constitutive equations, Eq. (3) provides a means for estimating the zero-shear viscosity by extrapolation to s_2 at $\dot{\gamma}=0$ [i.e., substituting the value of s_2 at zero shear into Eq. (3)]. Figure 3 demonstrates that there is generally good agreement between the zero-shear viscosities calculated by EMD simulations and those obtained via the aforementioned extrapolation. Moreover, Eq. (3), in conjunction with theories for structure under shear (see, e.g., [18–21,48]), provides a means to explore theoretically the rheology of fluids.

As a first test of the generality of the above structurally based constitutive equation, we also consider the monodisperse Lennard-Jones (LJ) fluid. Simulation details are the same as those presented above. For this model, quantities are reported in the standard LJ reduced form [40]. We investigate $T=0.5, 0.75, 1.0, 1.25$, $\phi_c=\pi\rho/6$ of 0.4 and 0.45, and shear rates in the range $\dot{\gamma}=0.005-1.0$. Under these conditions, both η and $-s_2$ are monotonically decreasing functions of shear rate. Figure 4 displays $\eta(\dot{\gamma})$ for the LJ fluid as a parametric function of $-s_2(\dot{\gamma})$. For convenience, we have scaled the viscosity by $\rho^{-2/3}T^{-1/2}$, as originally suggested by [1,2]. This scaling places the zero-shear viscosity of the dense LJ fluid onto a single curve. Again, we find that the shear-rate-dependent data is well described by Eq. (3). Also, as displayed in the inset to Fig. 4, there is good agreement between viscosities calculated from EMD simulations and those obtained from the structural extrapolation. These results, together with those for the SRA fluid, suggest that the structurally based constituative equation may hold for a variety of fluids, although more studies to verify this are warranted.

T.M.T., V.G., and W.P.K. acknowledge support of the National Science Foundation [Grants No. CTS-028772 (T.M.T.)

and No. CTS-0347381 (V.G.)] T.M.T. and V.G. acknowledge financial support of the Robert A. Welch Foundation. T.M.T. acknowledges support of the David and Lucile Packard Foundation and the Alfred P. Sloan Foundation. Simulations were performed at the Texas Advanced Computing Center.

[1] Y. Rosenfeld, Phys. Rev. A **15**, 2545 (1977).
[2] Y. Rosenfeld, J. Phys.: Condens. Matter **11**, 5415 (1999).
[3] M. Dzugutov, Nature (London) **381**, 137 (1996).
[4] S. Bastea, Phys. Rev. E **68**, 031204 (2003).
[5] R. Sharma, S. N. Chakraborty, and C. Chakravarty, J. Chem. Phys. **125**, 204501 (2006).
[6] J. Mittal, J. R. Errington, and T. M. Truskett, J. Phys. Chem. B **110**, 18147 (2006).
[7] J. Mittal, J. R. Errington, and T. M. Truskett, J. Chem. Phys. **125**, 076102 (2006).
[8] J. Mittal, J. R. Errington, and T. M. Truskett, Phys. Rev. Lett. **96**, 177804 (2006).
[9] J. R. Errington, T. M. Truskett, and J. Mittal, J. Chem. Phys. **125**, 244502 (2006).
[10] W. P. Krekelberg, J. Mittal, V. Ganesan, and T. M. Truskett, J. Chem. Phys. **127**, 044502 (2007).
[11] E. H. Abramson, Phys. Rev. E **76**, 051203 (2007).
[12] E. H. Abramson and H. West-Foyle, Phys. Rev. E **77**, 041202 (2008).
[13] G. Goel, W. P. Krekelberg, J. R. Errington, and T. M. Truskett, Phys. Rev. Lett. **100**, 106001 (2008).
[14] T. M. Truskett, S. Torquato, and P. G. Debenedetti, Phys. Rev. E **62**, 993 (2000).
[15] R. E. Nettleton and M. S. Green, J. Chem. Phys. **29**, 1365 (1958).
[16] J. H. Irving and J. G. Kirkwood, J. Chem. Phys. **18**, 817 (1950).
[17] H. H. Gan and B. C. Eu, Phys. Rev. A **45**, 3670 (1992).
[18] N. J. Wagner and W. B. Russel, Physica A **155**, 475 (1989).
[19] J. F. Brady, J. Chem. Phys. **99**, 567 (1993).
[20] R. A. Lionberger and W. B. Russel, J. Chem. Phys. **106**, 402 (1997).
[21] G. Szamel, J. Chem. Phys. **114**, 8708 (2001).
[22] K. Miyazaki, D. R. Reichman, and R. Yamamoto, Phys. Rev. E **70**, 011501 (2004).
[23] W. P. Krekelberg, T. M. Truskett, and V. Ganesan (unpublished).
[24] T. Eckert and E. Bartsch, Phys. Rev. Lett. **89**, 125701 (2002).
[25] K. N. Pham, A. M. Puertas, J. Bergenholtz, S. U. Egelhaaf, A. Moussaïd, P. N. Pusey, A. B. Schofield, M. E. Cates, M. Fuchs, and W. C. K. Poon, Science **296**, 104 (2002).
[26] J. Bergenholtz and M. Fuchs, Phys. Rev. E **59**, 5706 (1999).
[27] L. Fabbian, W. Gotze, F. Sciortino, P. Tartaglia, and F. Thiery, Phys. Rev. E **59**, R1347 (1999).
[28] K. Dawson, G. Foffi, M. Fuchs, W. Gotze, F. Sciortino, M. Sperl, P. Tartaglia, T. Voigtmann, and E. Zaccarelli, Phys. Rev. E **63**, 011401 (2000).
[29] E. Zaccarelli, G. Foffi, K. A. Dawson, S. V. Buldyrev, F. Sciortino, and P. Tartaglia, Phys. Rev. E **66**, 041402 (2002).
[30] F. Sciortino, Nat. Mater. **1**, 145 (2002).
[31] W. P. Krekelberg, J. Mittal, V. Ganesan, and T. M. Truskett, Phys. Rev. E **77**, 041201 (2008).
[32] A. M. Puertas, M. Fuchs, and M. E. Cates, Phys. Rev. Lett. **88**, 098301 (2002).
[33] A. M. Puertas, M. Fuchs, and M. E. Cates, Phys. Rev. E **67**, 031406 (2003).
[34] S. Asakura and F. Oosawa, J. Chem. Phys. **22**, 1255 (1954).
[35] J. M. Mendez-Alcaraz and R. Klein, Phys. Rev. E **61**, 4095 (2000).
[36] W. P. Krekelberg, V. Ganesan, and T. M. Truskett, J. Phys. Chem. B **110**, 5166 (2006).
[37] C. McCabe, C. W. Manke, and P. T. Cummings, J. Chem. Phys. **116**, 3339 (2002).
[38] P. J. Daivis and D. J. Evans, J. Chem. Phys. **100**, 541 (1994).
[39] D. J. Evans and G. P. Morriss, Phys. Rev. A **30**, 1528 (1984).
[40] D. C. Rapaport, *The Art of Molecular Dynamic Simulation*, 2nd ed. (Cambridge University Press, Cambridge, England, 2004).
[41] D. J. Evans and G. P. Morriss, *Statistical Mechanics of Nonequilibrium Liquids* (Academic, London, 1990).
[42] A. M. Puertas, E. Zaccarelli, and F. Sciortino, J. Phys.: Condens. Matter **17**, L271 (2005).
[43] A. M. Puertas, C. D. Michele, F. Sciortino, P. Tartaglia, and E. Zaccarelli, J. Chem. Phys. **127**, 144906 (2007).
[44] L. Berthier and J.-L. Barrat, J. Chem. Phys. **116**, 6228 (2002).
[45] V. Gopalakrishnan and C. F. Zukoski, J. Rheol. **48**, 1321 (2004).
[46] A. M. Puertas, M. Fuchs, and M. E. Cates, J. Chem. Phys. **121**, 2813 (2004).
[47] W. P. Krekelberg, V. Ganesan, and T. M. Truskett, J. Chem. Phys. **124**, 214502 (2006).
[48] D. Ronis, Phys. Rev. A **29**, 1453 (1984).